Supplementary Information for

Analyzing the Impact of Streamflow Drought on Hydroelectricity Production: A Global-Scale Study

Wenhua Wan[1,2], Jianshi Zhao[1], Eklavyya Popat[3], Claudia Herbert[3], Petra Döll[3,4]

[1] State Key Laboratory of Hydro-science and Engineering, Department of Hydraulic Engineering, Tsinghua University, Beijing, China

[2] School of Environment and Civil Engineering, Dongguan University of Technology, Guangdong, China

[3] Institute of Physical Geography, Goethe University Frankfurt, Frankfurt am Main, Germany

[4] Senckenberg Leibniz Biodiversity and Climate Research Centre Frankfurt (SBiK-F), Frankfurt am Main, Germany

Corresponding author: Petra Döll (p.doell@em.uni-frankfurt.de)

S1. Development of Global Hydropower Database (GHD)

S1.1 Compiling Hydropower Plant Records

Table S1 shows the four databases that served as the major original sources of constructing the GHD.

[INSERT Table S1 NEAR HERE]

Table S1. Open global power plant databases used for this study and their limitations.

Database	Provided data/ contribution focus	# of plants / total installed capacity	Limitations for HP simulation
World Power Plants Database	Plant name, geo-location[1], installed capacity, plant category (partly[2])	3215 0.7148 TW	Limited number of hydropower plants
URL: https://datasource.kapsarc.org/explore/dataset/world-power-plants-list/			
Global Power Plant Database version 1.3	Plant name, geo-location, commissioning year (partly), installed capacity, measured or estimated	7034 1.0458 TW	Plant category is not provided; some plants are not correctly located

	annual HP		
URL: http://datasets.wri.org/dataset/globalpowerplantdatabase			
Global Reservoir and Dam Database	Dam name, geo-location, commissioning year (partly), dam height (partly), storage capacity (partly), catchment and reservoir areas (partly), long-term mean streamflow (partly)	2495[3] n/a	No installed capacity info; no pumped-storage plants
URL: http://globaldamwatch.org/data/			
International Energy Statistics	Country-level total installed capacity, annual HP and total electricity generation for the years 1980–2018	n/a n/a	No data for individual hydropower plants
URL: https://www.eia.gov/beta/			

Notes. 1. Geo-location includes country as well as longitude and latitude in decimal degrees; 2. Not all plant records have this attribute, missing records in database are flagged with “-99” or left blank; 3. Only dams used for HP.

Regarding their different attributes and varying levels of accuracy, the plants were carefully matched across databases based on the given geolocations and plant attributes. There were 497 plants whose installed capacities were not provided by any data source. To estimate the missing installed capacity values, a power curve fitting between dam height and installed capacity was done. The obtained $N_{installed}$ estimations were then adjusted by multiplying a scaling factor such that the country total installed capacity became close to the EIA statistics. When other attributes such as hydraulic head, dam height or annual generation are reported, we included it directly in GHD.

Each record in GHD, as identified by a unique ID, typically represents a combined dam-reservoir-plant object. The geo-location of the plant represents the location of the main dam (or weir). If the dam straddles on the border between two countries, the hydropower plant is described by two plant records with the same nominal $N_{installed}$ but distinct actual $N_{installed}$, such as Moses-Saunders power dam (Canada/US). In addition, if the construction process of some plant took many years until all turbines were running and for some years, only a part of the turbines was producing hydropower, these plants are also marked as different records, such as the Itaipu Dam (Brazil/Paraguay, 18 plant records) and Yacyretá Dam (Paraguay/Argentina, 4 plant records).

S1.2 Date Specifications and Attribute Table of GHD

The GHD consists of two separate sheets provided in the xlsx format:

- "*1 GHD from multiple sources*" includes only data from other data sources;
- "*2 GHD with estimations*" includes also the estimations made to fill in missing H_{dam}, and derived from DDM30, WaterGAP 2.2d and HydroSHEDS.

Table S2 provides all attributes listed in the GHD. Depending on data availability and attribute necessity, some attribute fields are fully populated, while others remain incomplete.

[INSERT Table S2 NEAR HERE]

Table S2. Attributes provided in the GHD database.

Column title	Description	Symbol in article	# or occurrences
GHD_ID	Unique ID for each plant record and its associated dam/weir, reservoir		8716
Region	Name of the region; the six world regions are taken from the IHA regional classification, see Figure3c		8716
Country	Name of country		8716
Near_City	Name of nearest city		5314
Hydro_Dam	Name and alternative name of the dam structure		8716
Lon_P_X	Longitude of plant location in decimal degrees, an approximation of the dam location		8716
Lat_P_Y	Latitude of plant location in decimal degrees, an approximation of the dam location		8716
Install_Nom	Nominal installed capacity in MWs, the final or total installed capacity of a plant	nominated $N_{installed}$	8716
Install_Act	Installed capacity in MWs used for HP calculation	actual $N_{installed}$	8716

Hydro_Head	Maximum value of plant hydraulic head in meters	H_{max}	971
Dam_Hgt	Height of dam/weir in meters; the values in sheet "*1 GHD from multiple sources*" are observations while the missing records are filled by regression model estimation (see method in section 2.3) and listed in sheet "*2 GHD with estimations*"	H_{dam}	4169
Year_Open	Year in which the plant was first opened/commissioned, see also column "Timeline" below		5486
Gen_Gwhyr	Reported mean annual generation in gigawatt hours		7012
Install_qu	Indicates whether the installed capacity is obtained by power-curve fitting using column "Dam_Hgt"		435
Load_factor	Load factor in %, the ratio of the average electricity generated divided by the build-in capacity, also known as capacity factor or percentage full load.		36
Timeline	Operational status such as decommissioned in year x, retired, planned, refurbished		93
Category	Category of plant: Reservoir-storage, run-of-river, pumped-storage		2292
Catch_SKM	Area of upstream catchment draining into the reservoir in square kilometers		2561
Area_SKM	Surface area of reservoir in square kilometers		2457
Dis_Avg_CM	Long-term (1971−2000) average streamflow at dam location in liters per second derived from GRanD		2544
WaterGAP	Indicators whether the plant associated reservoir operation has been explicated simulated; If "Yes", then column "Storage"		716
River	Name of impounded river		2597
Res_Name	Name of reservoir or lake		740
Alt_River	Alternative name of impounded river		318
Main_Basin	Name of main basin		1147
Sub_Basin	Name of sub-basin		101
Alt_Year	Alternative year of dam construction		229
Cap_MCM	Representative maximum storage capacity of reservoir in million cubic meters	S_{max}	8714
Cap_Max	Reported 'maximum storage capacity' in million cubic meters derived from GRanD		796
Cap_Rep	Reported 'storage capacity' in million cubic meters		2347
Cap_Min	Minimum value of other reported storage capacities in million cubic meters		506
Depth_M	Average depth of reservoir in meters derived from GRanD		2531
Catch_Rep	Reported area of upstream catchment draining into reservoir in square kilometers		690
Arc_ID	Internal grid cell number derived from DDM30		8716
Lon_X	Longitude of plant location in 0.5 degrees derived from DDM30		8716

Lat_Y	Latitude of plant location in 0.5 degrees derived from DDM30		8716
Country_na	Name of Country of column "Arc_ID" derived from WaterGAP		8716
C_Area_Km2	Area of upstream catchment in square kilometers of column "Arc_ID" derived from WaterGAP		8716
Rout_Area	Watershed area in square kilometers of column "Arc_ID" derived from WaterGAP		8716
Basin_ID	Watershed ID		8716
Dis_Max	Long-term (1975−2016) mean highest monthly streamflow at dam location in meters per second derived from WaterGAP		8716
Dis_Min	Long-term (1975−2016) mean lowest monthly streamflow at dam location in meters per second derived from WaterGAP		8716
Storage_MCM	Long-term (1975−2016) mean reservoir storage in million cubic meters derived from WaterGAP	mean S_t	716
E_Head	Gridded elevation differences between the cells where the plant is located and downstream in meters (see method in section S1.2) derived based on HydroSHEDS database	H_{ele}	8716

Notes: Missing records are flagged with value "−99" or left blank.

S1.3 Citation

We kindly ask user to cite this article in any published material produced using the GHD.

S2. Probability Distribution Tests

Two sets of probability distribution tests have been implemented for SSI3 calculation (section 2.5.1) and HP risk analysis (section 2.6), using R package "gamlss" (Rigby & Stasinopoulos, 2005). This package contains more than 100 distributions, referred to as "gamlss.family". These distributions include, but are not limited to, normal, generalized normal, log-normal-3 parameter, gamma, Weibull, exponential, Pareto type II, generalized Pareto, Pearson type III, generalized extreme value, Gumbel, Poisson and t distributions.

In order to calculate SSI3, the distribution of 3-month averaged streamflow series were checked for all 67,420 grid cells for each calendar month. Twenty-five standard distributions in the gamlss.family have been tested. The Vuong and Clarke test (Clarke, 2007) was used to check the appropriateness of the chosen distributions by calculating P-values over all grid cells. The VC test suggests that the Pearson type III (PIII) is the most suitable choice since it can be accepted with P-values larger than 5% for 58.82% cases. Finally, the frequency analysis of hydrological drought was done by fitting a PIII distribution at each cell for each drought severity series.

The HP3 deficit events were checked for all 8428 conventional hydropower plants for 42 values, representing the annual maximum HP deficits for the period 1975–2016. The VC test indicates 76.5% ($\alpha = 0.05$) and 78.8% ($\alpha = 0.01$) of all plants accept KS test null hypothesis for Pareto type II distribution. The remaining 21.2% plants do not match any distribution because of the nearly identical HP deficit values of all 42 events.

S3. Performance of HP Simulation

[INSERT Figure S1 NEAR HERE]

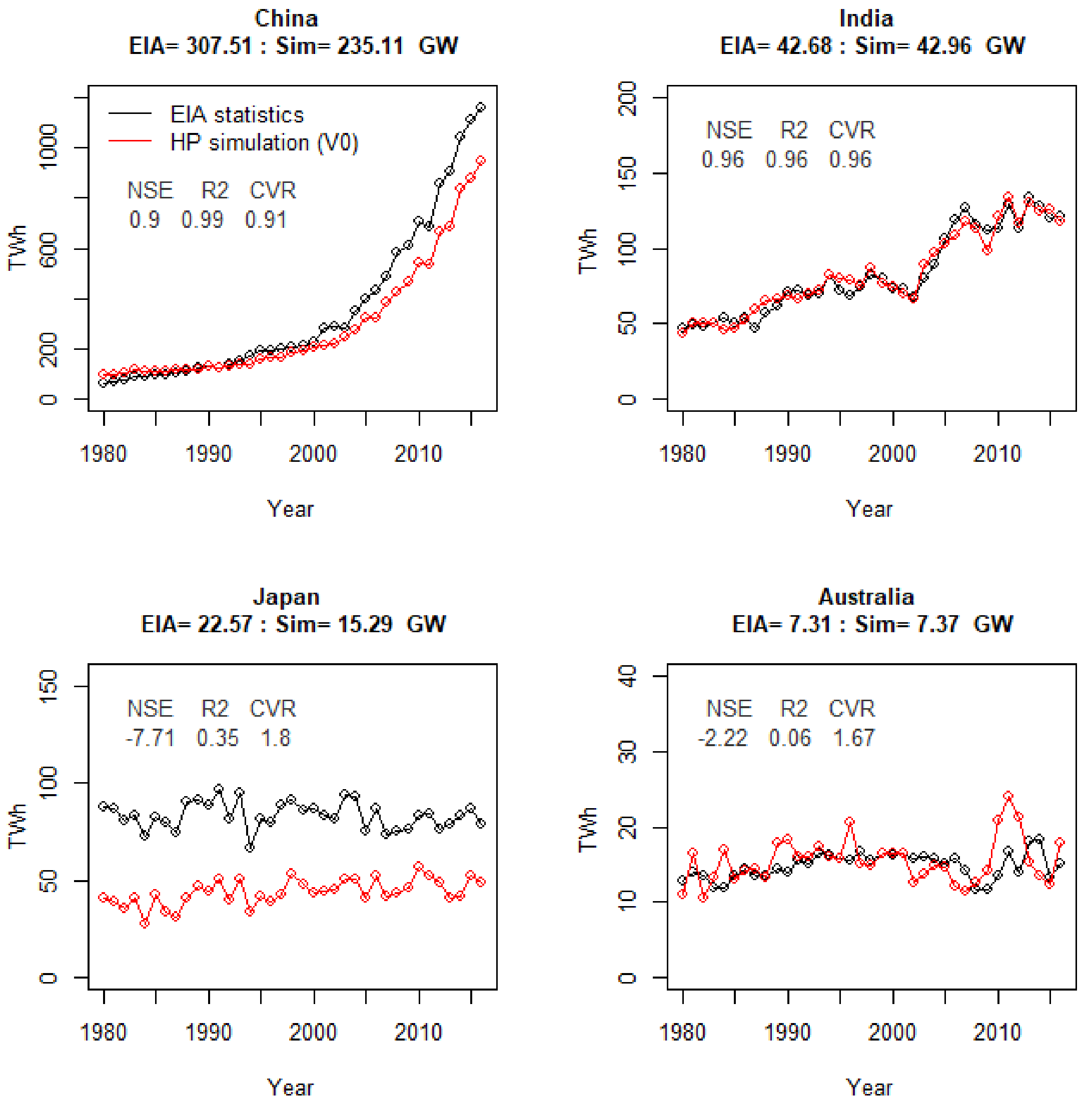

Figure S1. Comparison of the annual HP in simulation (red line) and EIA statistics (black line) for four representative countries for 1980–2016. The panel titles indicate the conventional installed capacities in 2016.

S4. Comparison of SSI3 based on observed and simulated streamflow

S4.1 Data and Methods

A limited data validation exercise was performed by comparing SSI3 based on streamflow observations provided by the Global Data Runoff Centre (GRDC) and WaterGAP 2.2d output (WFDEI-GPCC climate). The assessment included 183 globally distributed stations with continuous monthly streamflow observations between 1971 and 2000 and a minimum basin area of 20,000 m². The goodness-of-fit was evaluated based on (1) *NSE* for both SSI3 and streamflow, and (2) drought hazard classes.

Streamflow stations were selected from the 1319 calibration stations of WaterGAP 2.2d with continuous monthly streamflow observations between 1971 and 2000 and for basins larger than 20,000 km². The basin area of the resulting 183 stations (Figure S2) account for 24% of basin area covered by the all 1319 WaterGAP calibration stations (calibrated, hereinafter referred to as assessed basin area).

[INSERT Figure S2 NEAR HERE]

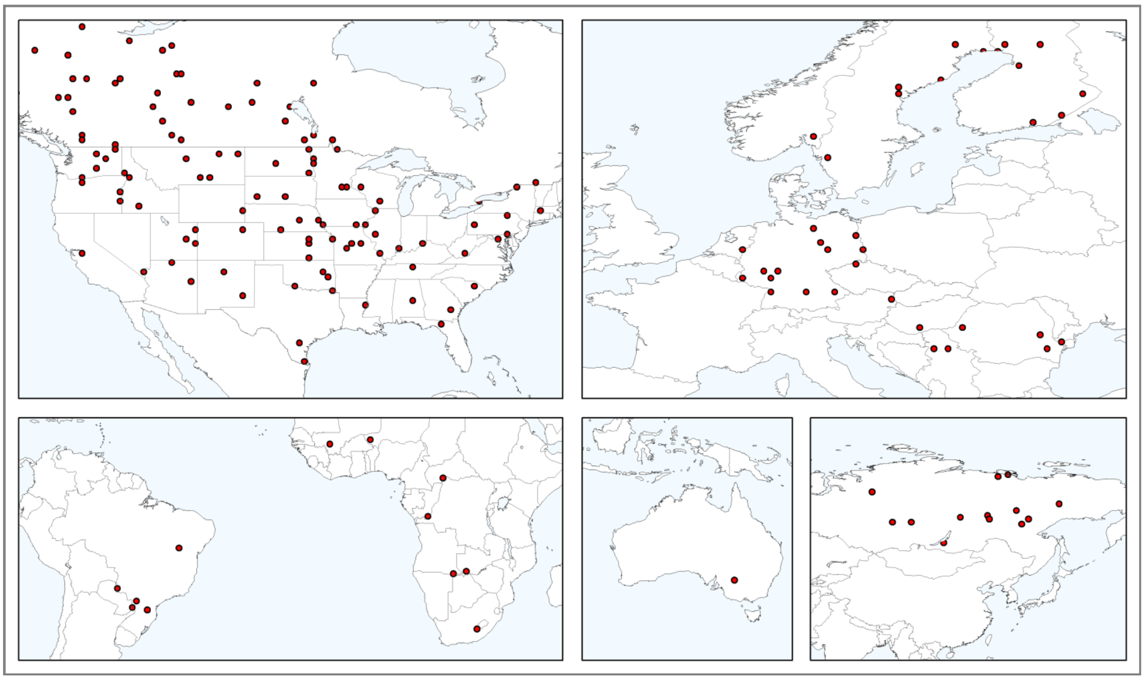

Figure S2. 183 GRDC stations with continuous monthly streamflow observations for the period 1971−2000 and basins larger than 20,000 km².

The Standardized Streamflow Index SSI was calculated for a 3-month averaging period for both simulated (SSI3(sim)) and observed (SSI3(obs)) streamflow using the R package “SCI” (Gudmundsson & Stagge, 2016) and the Pearson III distribution. To allow for a meaningful comparison, extreme SSI3 values were set to –2 and +2, respectively, with –2 considered as extreme drought (Agnew, 2000; McKee et al., 1993). The goodness-of-fit was evaluated based on the Nash-Sutcliffe efficiency (*NSE*) for both streamflow and SSI3. In addition, according to Agnew (2000), SSI3 less than −0.84 are classified as drought, and the agreement between simulated and observed classes was analyzed.

S4.2 Results

The *NSE* can range from −∞ to 1.0 (perfect fit), in which a negative value indicates that the mean of the observed data would have been a better predictor than the simulated time series (Krause et al., 2005). With a median of 0.5 and an interquartile range between 0.2 and 0.7, the *NSE* for SSI3 (Figure S3, left) indicates a moderate agreement among all 183 stations. The goodness-of-fit is very similar for monthly time series of streamflow (*NSE*(Q)), albeit with slightly more values closer to and below zero (lower quartile of 0.14). *NSE*(SSI3) is larger than *NSE*(Q) at 100 stations representing 41% of the assessed basin area. Both *NSE*s are larger than 0.7 at 25 stations (19% of assessed area), which are located in Central and Eastern Europe (twelve stations), the United States (ten stations), Brazil (two stations at Iguaçu River), and South Africa (one station at Orange River).

[INSERT Figure S3 NEAR HERE]

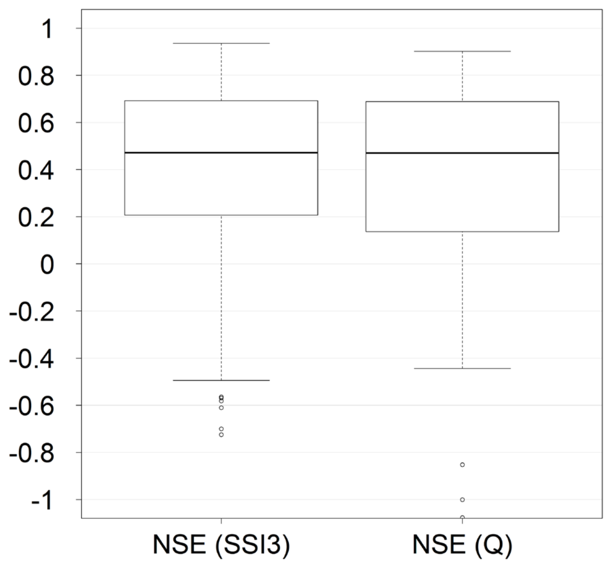

Figure S3. Nash-Sutcliffe efficiency (*NSE*) for SSI3 and streamflow Q for 183 selected stations for the period 1971–2000.

Among all stations, the agreement between simulated and observed drought hazard classes ranges between 29 to 88% of all 360 months (Figure S4 and Table S3) and is mostly attributable to class 1 (i.e. normal conditions, 28 to 78% of all months). At a large number of stations (83% of the assessed basin area), simulated and observed SSI3 values fall into the same class in 70% of the time.

[INSERT Figure S4 NEAR HERE]

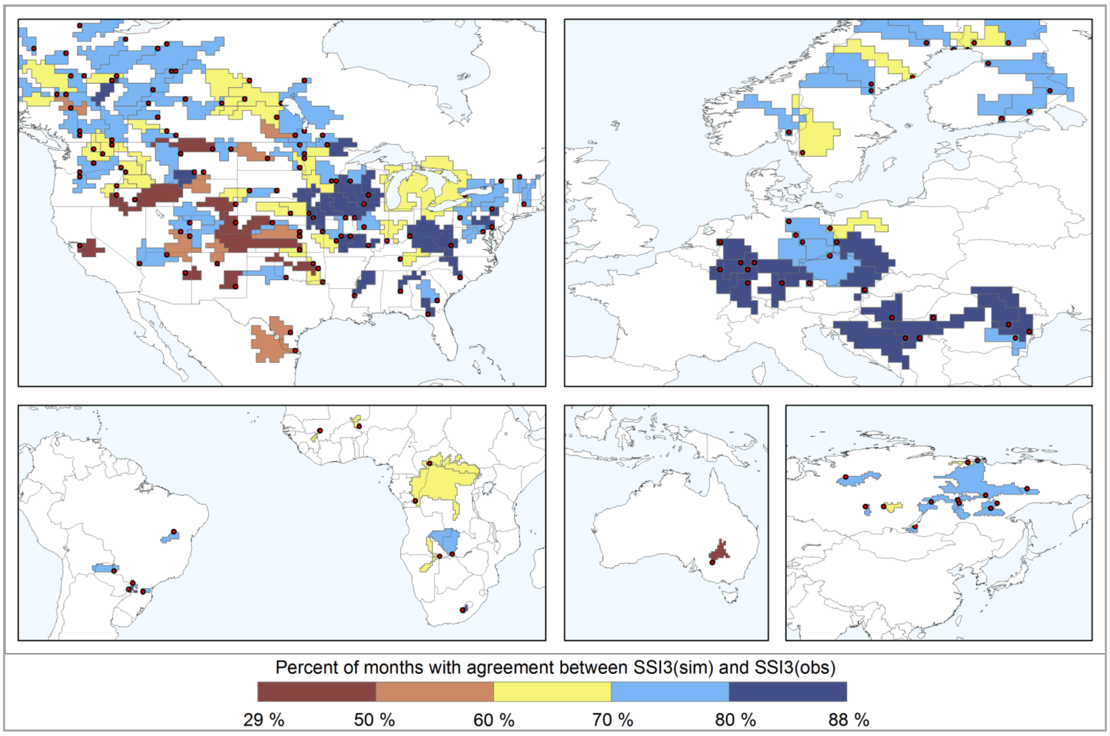

Figure S4. Agreement between simulated and observed drought hazard classes at 183 selected stations and associated basins: percent of months in the period 1971−2000 where values of SSI3(sim) and SSI3(obs) fall into the same drought hazard class according to Agnew (2000).

[INSERT Table S3 NEAR HERE]

Table S3. Number (and percent) of stations and percent of assessed basin area with a certain percentage of agreement between simulated and observed drought hazard classes over all months during 1971−2000.

Percent of months with agreement	Absolute number of stations (percent of all 183 stations)	Percent of assessed basin area
> 29 to 50%	12 (7%)	3%
> 50 to 60%	9 (5%)	3%
> 60 to 70%	38 (21%)	11%
> 70 to 80%	87 (48%)	57%
> 80 to 88%	37 (20%)	26%

Figure S5 shows simulated and observed streamflow differences for three illustrative hydrological stations in Germany between 1990 and 2016. Both the Danube and the Rhine belong to Europe’s major rivers; the Main is a tributary of the Rhine.

Comparing SSI3 time series based on streamflow observations and WaterGAP simulations, the 2003 drought is well represented by WaterGAP in case of the Rhine and Danube stations but overestimated for the Main.

[INSERT Figure S5 NEAR HERE]

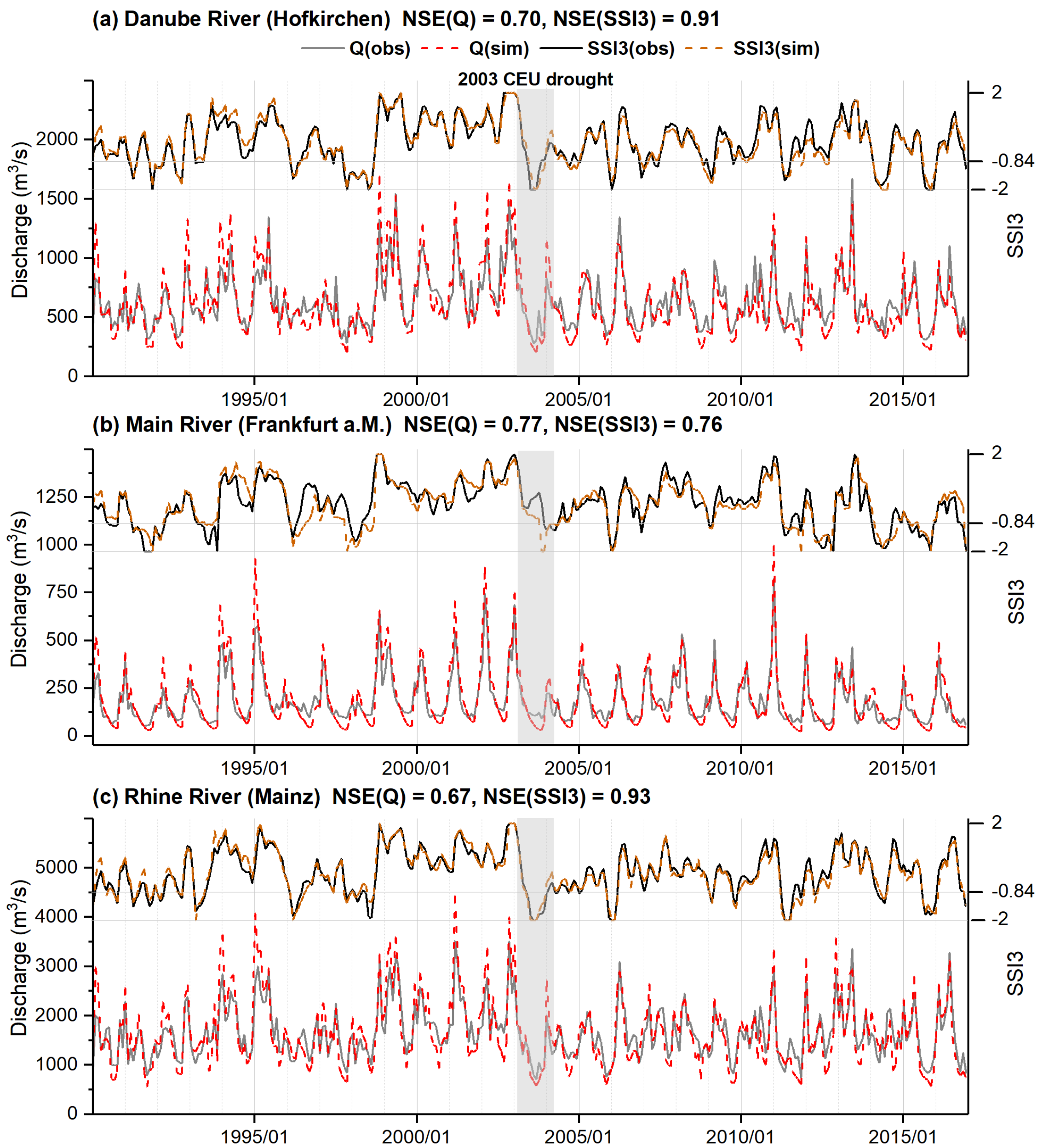

Figure S5. Simulated and GRDC observed monthly streamflow (1990–2016) and the SSI3 values (based on data from a reference period from 1971 to 2016) at three German stations: Danube River at Hofkirchen (a), Main River at Frankfurt am Main (b), and

Rhine River at Mainz (c). The corresponding geo-locations are (48.68, 13.12), (50.11,8.72) and (50.00,8.28), respectively. Extreme SSI3 values are set to −2 and +2. The *NSE* is given for streamflow (Q) and SSI3 time series.

S5. HP Anomaly during 2003 Drought in Central Europe

The standard z-scores was introduced to quantify how unusual the HP during a drought event is, as compared with the "normal" state for a specific cell/country. The z-score is computed by standardizing the variable via mean and standard deviation

$$z = \frac{\sum_t \sum_i HP_{i,t} - \mu}{\sigma} \tag{1}$$

where $HP_{i,t}$ is the HP of power plant i located in a specific cell/country for time step t during a streamflow drought event, μ and σ are the mean and standard deviation over the same period and region of historical HP.

[INSERT Figure S6 NEAR HERE]

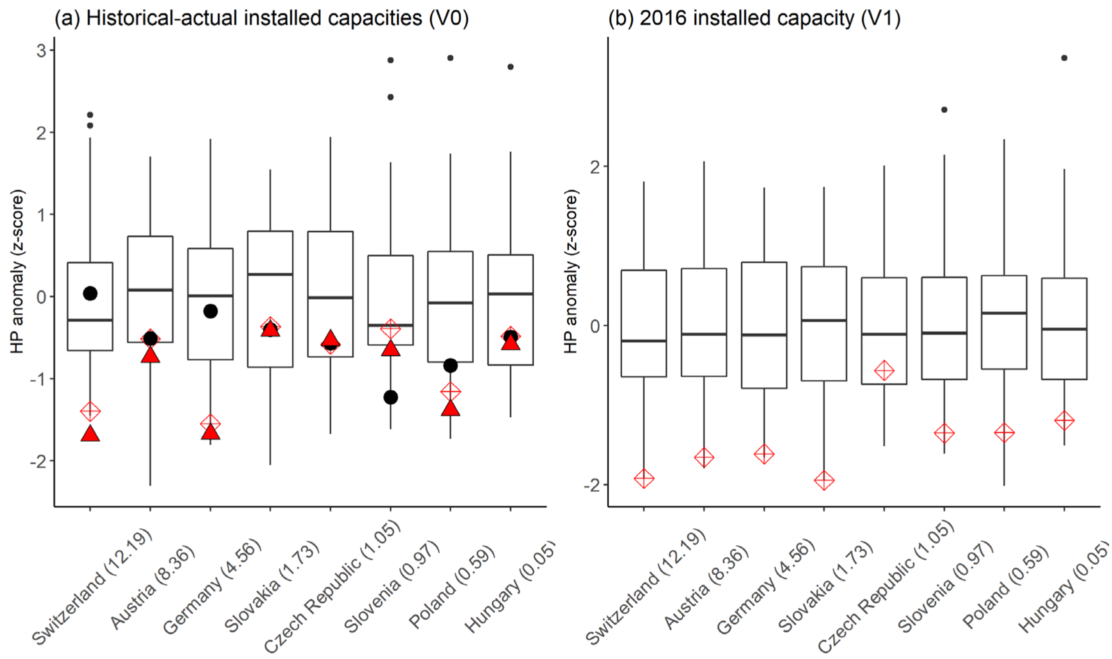

Figure S6. Z-score box-plot of aggregated HP over the same 2003 CEU drought months (02.2003–03.2004) for years 1980–2016. (a) is based on the HP in model variant V0 and (b) in V1. Triangles and circles in (a) are the same as that in Figure 7e, 7f. Red diamond pluses show the simulated HP anomalies during 2003 CEU drought.

S6. Evaluation for Reservoir Storage in the US

The WaterGAP simulated reservoir storage was compared to gauge observations for the five large hydropower reservoirs in the United States (Fort Peck, Garrison, Oahe, Big Bend, and Gavins Point). Monthly observed reservoir storage was obtained from the US Army Corps of Engineers and the US Bureau of Reclamation (https://www.nwd-mr.usace.army.mil/rcc/projdata/projdata.html). The storage estimates are found highly correlated with observations in Fort Peck, Garrison and Oahe (R^2= 0.38 to 0.68), but very low in Big Bend and Gavins Point (R^2<0.1). In the long run, WaterGAP underestimates the storage in Fort Peck reservoir for about 21%, Big Bend for 23% and Gavins Point for 33%, while slightly overestimates the storages in the other two reservoirs.

[INSERT Figure S7 NEAR HERE]

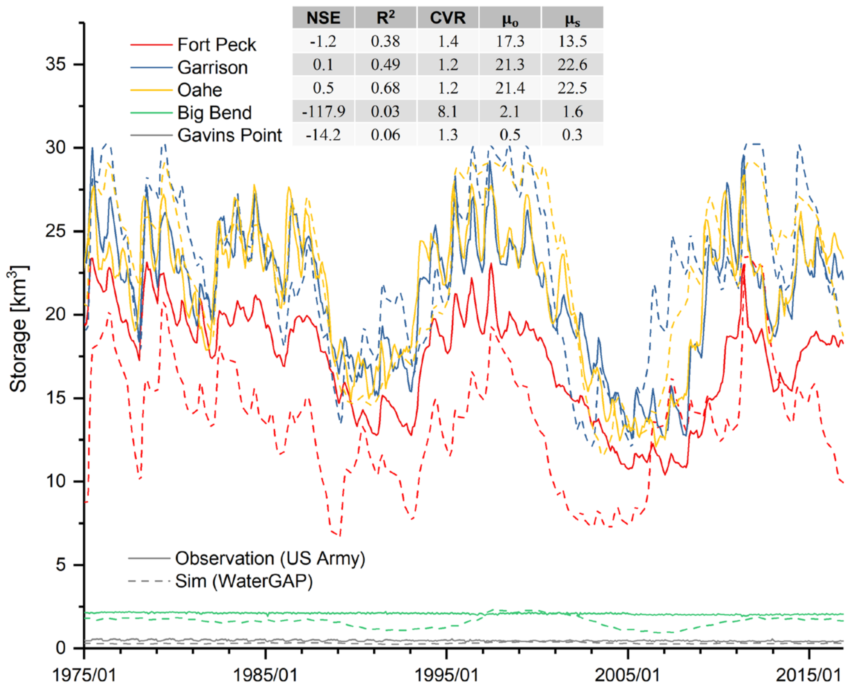

Figure S7. Evaluation of the reservoir storage from WaterGAP simulation compared to gauge observations for five US reservoirs.

S7. Relation between Streamflow Drought and HP Reduction

[INSERT Figure S8 NEAR HERE]

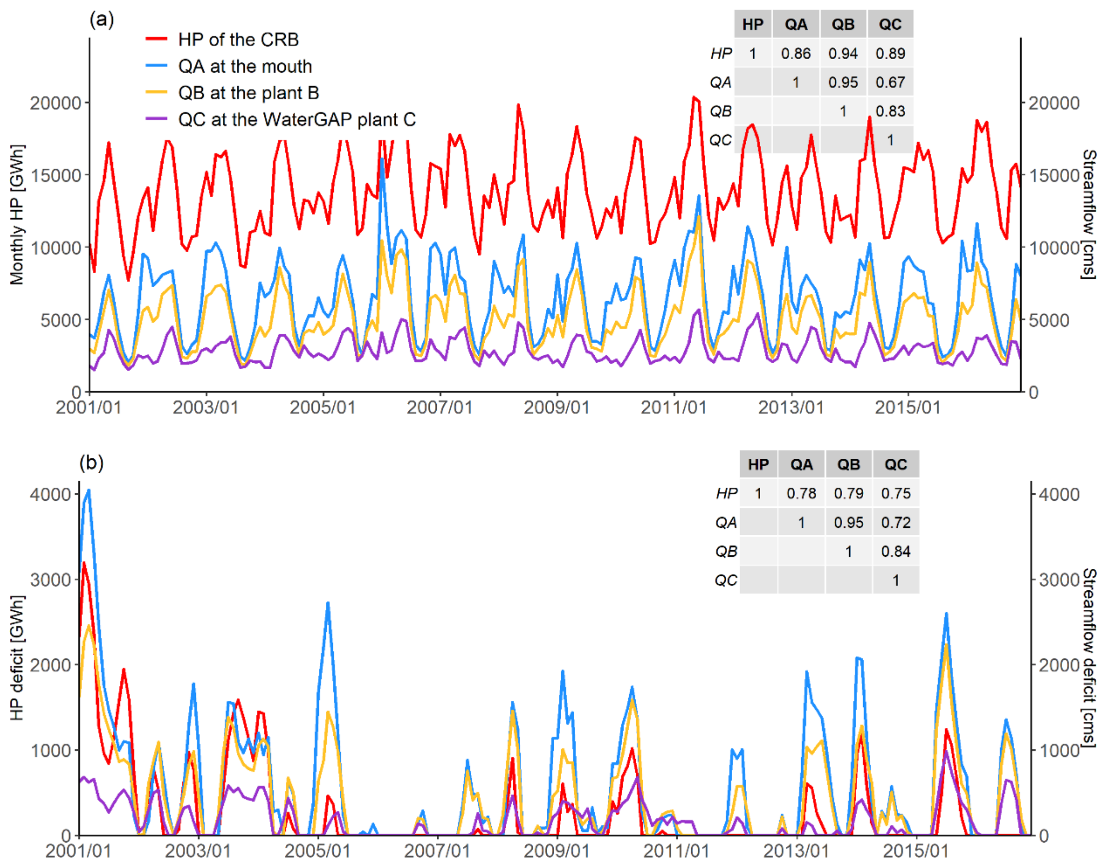

Figure S8. Comparison of the simulated HP for the whole Columbia River Basin, and streamflow at the cells A, B and C as shown in Figure 10 (a), and the respective deficits (b). The table on the right corner of each panel lists the matrix of correlation coefficients.